South African Journal of Chemical Engineering 38 (2021) 78–89

Contents lists available at ScienceDirect

South African Journal of Chemical Engineering

journal homepage: www.elsevier.com/locate/sajce

Optimal removal of diclofenac and amoxicillin by activated carbon prepared from coconut shell through response surface methodology

Mohamed M. Arêmou Daouda [a,b,*], Akuemaho V. Onésime Akowanou [a], S. E. Reine Mahunon [a], Chris K. Adjinda [a], Martin Pépin Aina [a], Patrick Drogui [c]

[a] Laboratoire des Sciences et Techniques de l'Eau et de l'Environnement, Institut National de l'Eau, Université d'Abomey-Calavi, Bénin,West Africa
[b] International Chair in Mathematical Physics and Applications, (ICMPA-UNESCO Chair), Université d'Abomey-Calavi, Bénin,West Africa
[c] Institut National de la Recherche Scientifique (INRS Eau Terre et Environnement), Université du Québec, 490 rue de la Couronne, Québec City, Canada

ARTICLE INFO

Keywords:
Coconut shells
Amoxicillin
Diclofenac sodium
Activated carbon
Response surface methodology

ABSTRACT

Agricultural residues like coconut shell are widely available in Benin Republic and can be used as adsorbent. In this study, we determine the limits of pharmaceutical substances adsorption by activated carbon from coconut shells. The synthesis of this adsorbent was optimized by the Response Surface Methodology (RSM) with two factors: the impregnation ratio IR and activation temperature. The iodine value was considered as the performance (response) parameter of this synthesis. After characterizing the prepared activated carbon, adsorption tests were performed on diclofenac sodium (DCF) and amoxicillin (AMX) by varying the contact time and the adsorbate-adsorbent ratio R_{ads}. The synthesis results showed that the optimal physicochemical properties of the activated carbon were observed at 740 °C with phosphoric acid (IR = 1.66). Under these optimal conditions, the activated carbon from the coconut shells presented a large microporous specific surface ($S_{BET} = 437\ m^2/g$ and $V_{micro} = 0.21\ cm^3/g$), optimal iodine adsorption (930.28 mg/g), amorphous and low heterogeneous chemical composition. In addition, the prepared activated carbon was an excellent adsorbent for the removal of the pharmaceutical substances studied. The experimental adsorption data followed the Langmuir isotherm and the pseudo first-order kinetic model. However, the efficiency varied depending on the nature of the adsorbate and the adsorbate-adsorbent ratio was the main limiting factor in the adsorption process. Optimal elimination greater than 98% was noticed with $R_{ads} = 0.10$ and a contact time of 15 min (90 min) for DCF (AMX). However, we noticed the complete elimination of AMX (DCF) for $R_{ads} \leq 0.075$ ($R_{ads} \leq 0.040$). It was observed that the removal efficiency of pollutant was not defined by the adsorption rate constant but the reactivity with the adsorbent.

1. Introduction

The presence of emerging pollutants, even at low concentrations, highly threatens the aquatic environment. Commonly referred to as micropollutants, they come directly or indirectly from domestic, hospital, industrial wastewater and runoff water (Luo et al., 2014; Mailler et al., 2017). Among the micropollutants, those of pharmaceutical origin constitute a significant concern because they are the most common and are at risk for aquatic biota (Busch et al., 2016; Deblonde et al., 2011). Their toxicity varies according to the therapeutic class and the active principle. For example, diclofenac is very toxic to living organisms (Shao et al., 2019) while amoxicillin only affects cyanobacteria (González-Pleiter et al., 2013). These two drugs are among the most present pharmaceutical micropollutants in the environment (Cizmas et al., 2015; Verma and Haritash, 2020; Xiong et al., 2019).

In general, conventional treatment methods are very selective and ineffective in removing pharmaceutical micropollutants (Falås et al., 2016; Margot et al., 2013; Pasquini et al., 2014). New treatment methods and techniques complementary to conventional methods are often required. Advanced treatment techniques developed to remove pharmaceutical micropollutants from the environment include adsorption, ozonation, electrochemical-oxidation, photodegradation, etc. However, considering the ease of implementation, adsorption is the most cost-effective treatment technique (Kovalova et al., 2013). And activated carbon is the most studied adsorbent because of its treatment efficiency and its affordable cost (Burakov et al., 2018). The main advantages of using activated carbon are its high surface area (Suhas et al., 2016) and its ease of regeneration using the sun (Miguet et al., 2016) .

* Corresponding author.
E-mail address: mouharrab@yahoo.fr (M.M.A. Daouda).

https://doi.org/10.1016/j.sajce.2021.08.004
Received 31 December 2020; Received in revised form 8 July 2021; Accepted 17 August 2021
Available online 20 August 2021

Table 1
Properties of amoxicillin and diclofenac.

Parameter	Amoxicillin (AMX)	Diclofenac sodium (DCF)
Therapeutic class	Antibiotic	Anti-inflammatory
Molecular structure	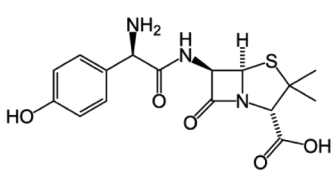	
Molecular formula	$C_{16}H_{19}N_3O_5S$	$C_{14}H_{10}Cl_2NNaO_2$
CAS number	26787-78-0	15307-79-6
Molar mass (g/mol)	365.4	318.13
Purity	99 %, Pharmaquick-Benin	99¨%, Macklin
Solubility in water at 20°C (g/L)	3.43	50

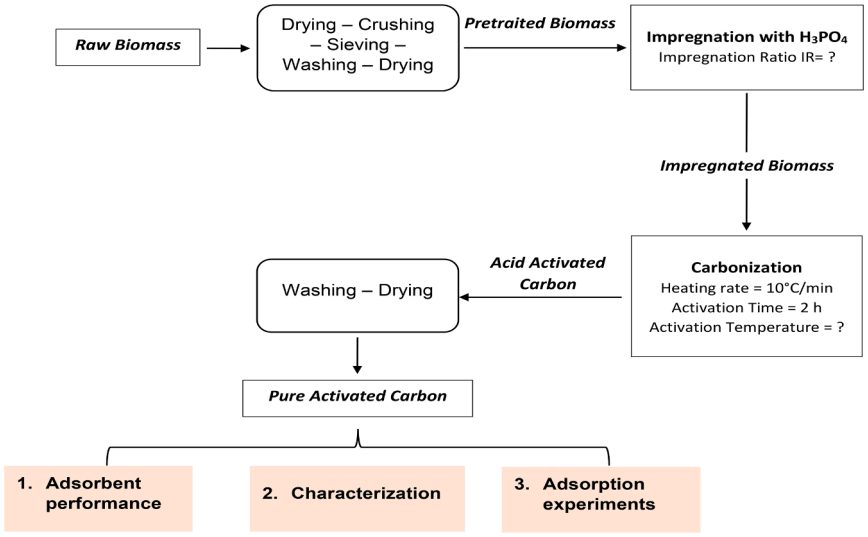

Fig. 1. The activated carbon preparation process.

Chemical activation is more studied in the literature than physical activation and presents the best final product in terms of quality and cost ratio (Heidarinejad et al., 2020; Jodeh et al., 2016). An Acid or base reagent is usually used as activating agent (Budi et al., 2017). The most effective activated agents are potassium hydroxide (Azmi et al., 2015; Li et al., 2017) and phosphoric acid (Balogoun et al., 2015; Gratuito et al., 2008; Gueye et al., 2014; Heidarinejad et al., 2020). The reason is the high potential of macromolecule fragmentation and pore creation by $PO_4^{3-}$and K^+ions (Marsh and Rodriguez-Reinoso, 2006). The main disadvantage of activation with potassium hydroxide is its toxic effect and the low yield of charcoal induced (Hui et al., 2015) while phosphoric acid is environment friendly and cost-effective (Jawad et al., 2020; Sun et al., 2016).

In general, the quality of activated carbon depends on three main factors: the impregnation ratio, the temperature of activation and the duration of activation (Das and Mishra, 2017). Using response surface methodology (RSM), these main factors can be optimized to prepare activated carbon (As et al., 2015; Asfaram et al., 2015; Senthilkumar et al., 2017; Tan et al., 2008a). According to this method, the impregnation ratio and the activation temperature are the most significant factors (Vargas et al., 2010). The adsorption process can be modeled using Langmuir and Freundlich isotherms which are widely used because of the simplicity of their mathematical expression (Lesaoana et al., 2019; Moussavi et al., 2013; Nayl et al., 2017). Combined with pseudo first-order, pseudo second-order or intra-particle diffusion models, Langmuir and Freundlich isotherms best express adsorption of activated carbon (Mahmood and Abdulmajeed, 2017; Nekouei et al., 2015; Putra et al., 2009). The option of kinetic study via a numerical model of fluid dynamics is possible but its accuracy is minimal (Maddodi et al., 2020). However, the appropriate model depends on the

Table 2
Experimental design matrix and results.

N°	Experiment plan Codes variables X_1	X_2	Actual variables x_1	x_2	Response Iodine value (mg/g) Exp	RSM
Factorial Design						
1	−1	−1	1	500	439.82	480.14
2	1	−1	2	500	658.86	645.36
3	−1	1	1	700	717.69	690.96
4	1	1	2	700	949.69	869.15
Central Composite Design						
5	−1.414	0	0.793	600	454.10	436.16
6	1.414	0	2.207	600	620.81	678.98
7	0	−1.414	1.5	458.579	658.86	631.57
8	0	1.414	1.5	741.421	871.37	938.89
9	0	0	1.5	600	821.80	835.40
10	0	0	1.5	600	815.63	835.40
11	0	0	1.5	600	831.57	835.40
12	0	0	1.5	600	870.48	835.40
13	0	0	1.5	600	837.54	835.40

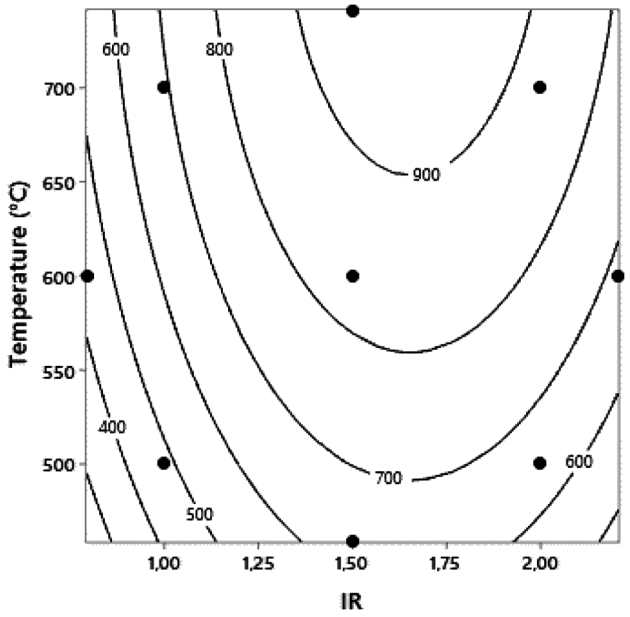

Fig. 2. Interaction effect of activation temperature and impregnation ratio on iodine value.

Table 3
ANOVA for response surface quadratic model for iodine adsorption value.

Source	Degree of freedom	Sum of square	Mean square	F-value	p-value
Model	5	288,040	57,608	20.32	**0.000**
X_1	1	58,962	58,962	20.80	**0.003**
X_2	1	94,446	94,446	33.31	**0.001**
X_1^2	1	134,246	134,246	47.35	**0.000**
X_2^2	1	4378	4378	1.54	0.254
X_1X_2	1	42	42	0.01	0.907
Pure error	7	19,845	2835		
Model summary	$R^2 = 93.55\%$, $R_{adj}^2 = 88.95\%$, $R_{Pred}^2 = 57.46\%$, $CV = 7.24\%$				

pollutant and the nature of the activated carbon (Jodeh et al., 2016; Tomul et al., 2019). The effectiveness of the treatment is indirectly dependent not only on the nature of the pollutant but also on the

Table 4
Validation of model and optimum operating conditions.

Solution proposed by Minitab Software Solution	IR	Temperature (°C)	Iodine value (mg/g)	Desirability composite
1	1.664	741.42	953.61	1
Experimental results				
Tests	**IR**	**Temperature (°C)**	**Iodine value (mg/g) Theoretical**	**Experimental**
1	1.660	740.00	953.61	921.01
2				915.84
3				953.99
Average	1.660	740.00	953.61	930.28

Table 5
Comparison of iodine value of some coconut tree biomass based activated carbon.

Precursor	Activated agent	Iodine value (mg/g)	References
Coconut shell	H_3PO_4	930.28	This study
Coconut shell and municipal sludge	KOH	698.37 798.31	(Liang et al., 2020) (Yang et al., 2019)
Coconut shell	H_3PO_4	787	(Balogoun et al., 2015)
Coconut shell	Self-activation	1280	(Sun et al., 2017)
Coconut leaf	H_2SO_4	263	(Jawad et al., 2016)
Coconut leaf	KOH	538	(Rashid et al., 2016)
Coconut leaf	H_3PO_4	909	(Jawad et al., 2017b)

Table 6
Intrinsic characterization of activated carbon.

Analysis	Parameters (%)	Raw biomass	Activated carbon
Macromolecular composition	Extractible	18.60	
	Cellulose	34.10	
	Hemicellulose	14.10	
	Lignin	32.80	
Immediate analysis	Volatile matter	80.84	21.76
	Fixed carbon	18.73	76.03
	Ash	0.43	2.22
Ultimate analysis	Carbon	45.28	60.00
	Hydrogen	4.05	0.00
	Oxygen	42.70	1.43
	Nitrogen	0.20	1.22
	Phosphorus	0.00	15.21

characteristics of the activated carbon (Mailler et al., 2016).

Several lignocellulosic precursors like biomass waste of coconut tree have been used to prepare activated carbon (Freitas et al., 2019; Jawad et al., 2017a). For this study, coconut shells were chosen because of their great availability in Benin Republic (Balogoun et al., 2015). The efficiency of activated carbon from coconut tree waste has been widely proven on standard pollutants such as methylene blue (Jawad et al., 2015) and phenol (Bazrafshan et al., 2016). Few researches present the applications of activated carbon on pharmaceutical pollutant (González-García, 2018). Furthermore, studies on the adsorption of more than one pharmaceutical molecule do not provide the same optimal condition for all the studied molecules. In this particular study, the optimal removal conditions were assessed to meet both Diclofenac and Amoxicillin optimal removal. The study's goal was the preparation of activated carbon from coconut shells for the adsorption of amoxicillin and diclofenac. We used dimensionless parameter which express the

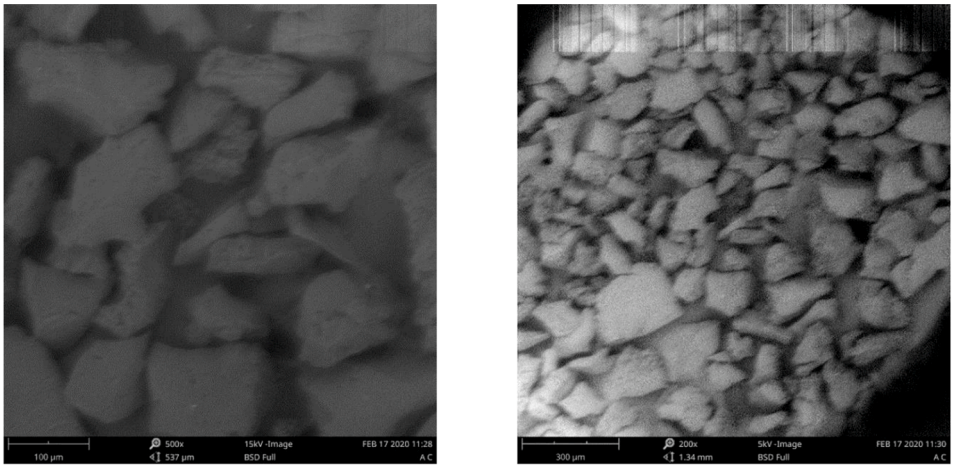

(a)

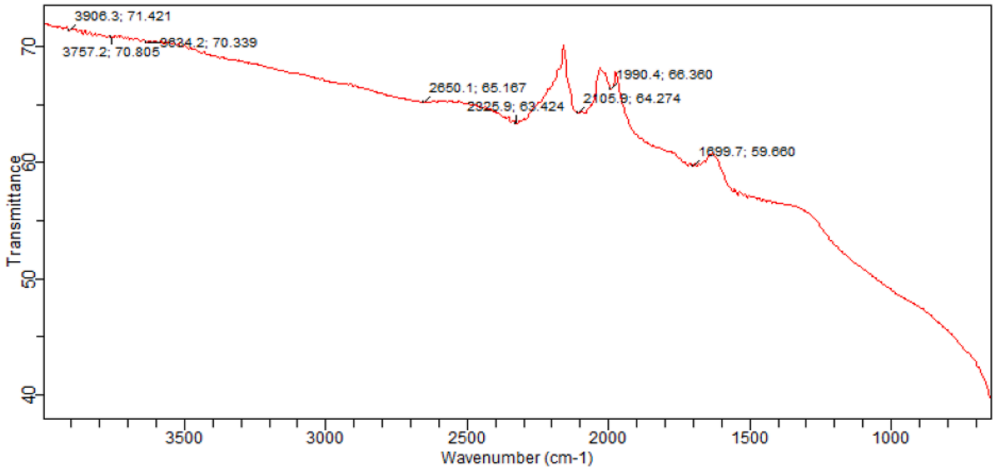

(b)

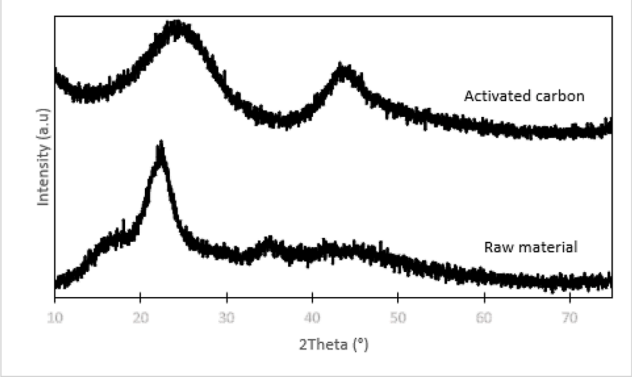

(c)

Fig. 3. Intrinsic characterization of activated carbon - a) SEM, b) FTIR and c) XRD.

Table 7
Comparison of the textural characteristics of activated carbon from different agricultural residue.

Precursor	Activated agent	S_{BET} (m^2/g)*	V_{micro} (cm^3/g)*	d_p (nm)*	References
Coconut shell	H_3PO_4	437	0.21	2.13	This study
Shea shell	H_3PO_4	477	0.21	–	(Telegang Chekem, 2017)
Peanut shell	H_3PO_4	395.80	0.21	3.53	(Georgin et al., 2016)

* : determination according to BJH Method.

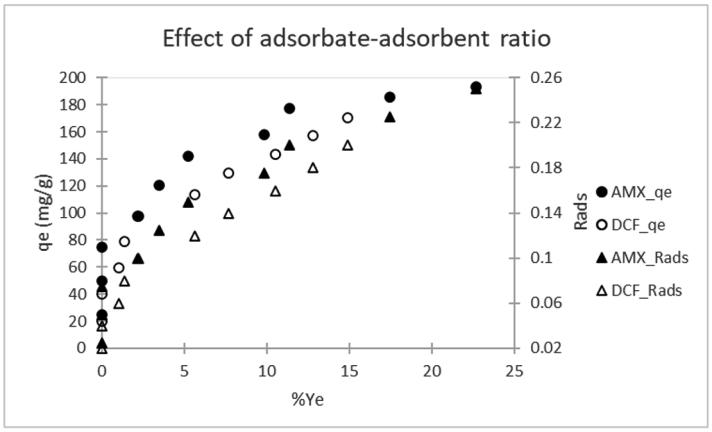

(a)

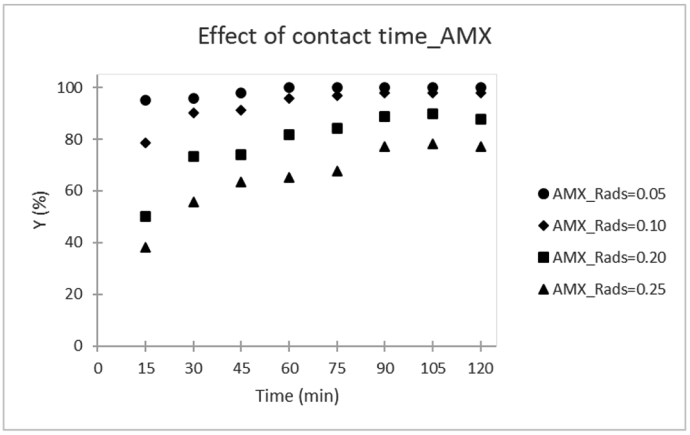

(b)

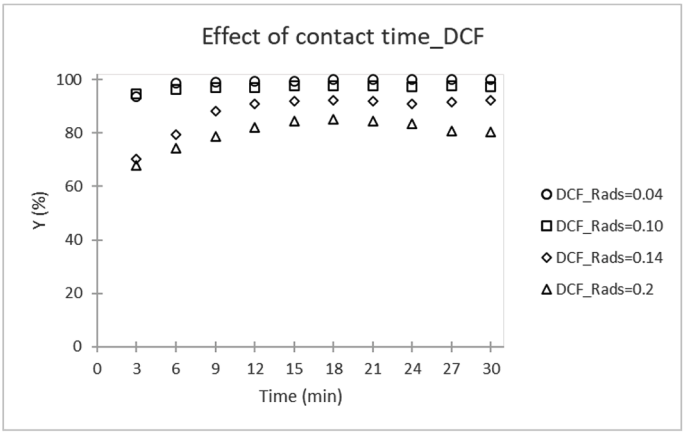

(c)

Fig. 4. Effect of initial R_{ads} (a), contact time for AMX (b) and DCF (c).

initial concentration of adsorbent and adsorbate to explore adsorption.

2. Materials and methods

2.1. Materials

The activated carbon used in this study was prepared from coconut shells. These shells collected from a local cooperative were previously dried in the sun and then crushed. The 0.5 to 2 mm particle size fraction was washed and dried at 105 °C for 24 h in the drying oven. Adsorption was performed on amoxicillin and diclofenac sodium, whose characteristics and chemical structure are presented in Table 1 All chemical products are of an analytical class and the solutions were prepared with distilled water.

2.2. Preparation of activated carbon and statistical approach to the experimental design

The activated carbon was prepared using the chemical activation method: pretreatment, impregnation, carbonization and washing (Fig. 1).

The impregnation consisted of heating under reflux for 2 h of the

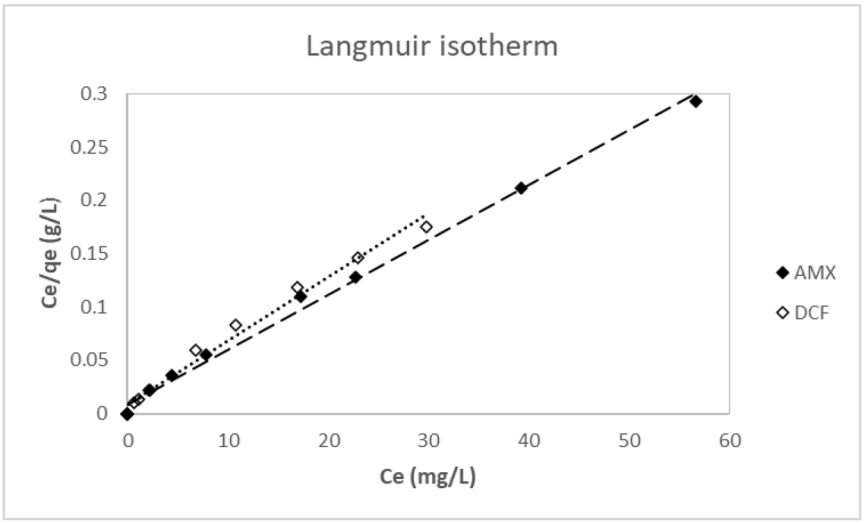

(a)

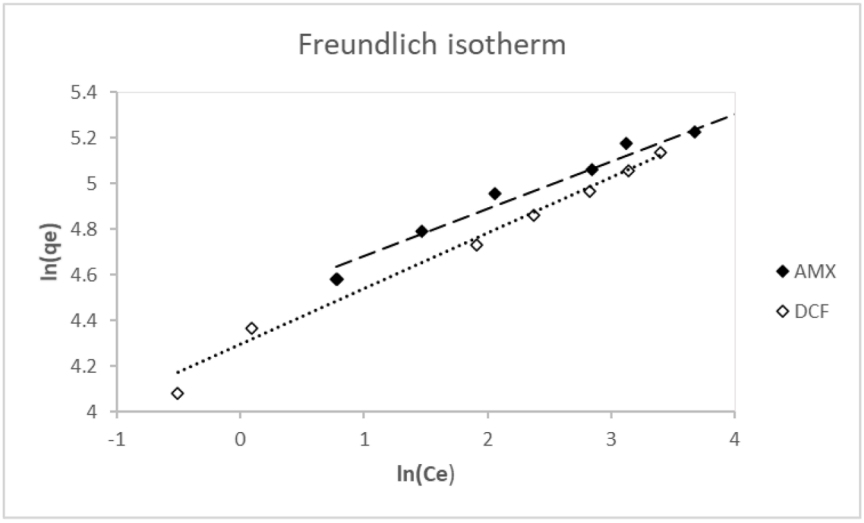

(b)

Fig. 5. Langmiur (a) and Freundlich (b) isotherms.

pretreated biomass and phosphoric acid solution mixture in a liquid/solid ratio equal to 2. The impregnated mixture was previously filtered and dried at 105 °C for 48 h before carbonization.

After carbonization, the activated carbon was washed with distilled water at a pH close to neutrality, then dried at 105 °C for 24 h. A grinding operation allowed the activated carbon grain charcoal to be refined to a particle size between 0.07 and 0.2 mm.

In this study, the RSM was used to optimize the preparation of activated carbon. This method enables the assessment by a statistical model of the influence of the factors on the studied answers. Two factors (variables) were considered: impregnation ratio IR (x_1 ranging from 1 to 2) and activation temperature (x_2 ranging from 500 °C to 700 °C). The factorial design of two-level square order completed by a central composite design with 4 axial tests and 5 repeat points at the center for a total of 13 tests were conducted for this statistical modeling (Table 2). Between the two most considered responses during the activated carbon preparation, the methylene blue value and the iodine value (Baçaoui et al., 2001; Bestani et al., 2008; Itodo et al., 2010), iodine value was adopted as the experimental design response, as it reveals the adsorption capacity of micropores (Budnyak et al., 2018; Patnukao and Pavasant, 2008). Experimental data were modeled by second-order polynomial regression:

$$Y = b_0 + \sum_{i=1}^{k} b_i X_i + \sum_{i=1}^{k} b_{ii} X_i^2 + \sum_{j \neq i} \sum_{i=1}^{k} b_{ij} X_i X_j + e_i \quad (1)$$

where y is the predicted response (iodine value) $X_i$andX_j are coded variables with $k = 2; b_0, b_i, b_{ii}$ and b_{ij} represent the coefficients of interception regression, linear terms, quadratic terms and interaction terms respectively

The variance analysis was performed to determine the statistical significance and influence of the independent and interactive variables of the model and the optimal condition for the preparation of the activated carbon. MINITAB 19 Statistical Software was used to conduct the experiment design.

Table 8
Isotherm parameters for AMX and DCF adsorption on activated carbon.

Isotherms	Adsorbate	Parameters	Values
Langmuir	Amoxicillin	q_{max}(mg /g)	192.31
		R_L	0.0052
		K_L(L /mg)	0.6420
		R^2	0.9946
	Diclofenac sodium	q_{max}(mg /g)	166.67
		R_L	0.0060
		K_L(L /mg)	0.7143
		R^2	0.9846
Freundlich	Amoxicillin	$K_F(mg/g)(mg/L)^{-\frac{1}{n}}$	87.94
		n	4.8286
		R^2	0.9693
	Diclofenac sodium	$K_F(mg/g)(mg/L)^{-\frac{1}{n}}$	73.38
		n	4.0967
		R^2	0.9765

2.3. Characterization of the precursor and the adsorbent

The macromolecular composition which provides information on the lignocellulosic biomass content was determined by the Van Soest titration technique (Godin et al., 2011; Pellerin, 2002). The rate of dry volatile matter (in ATG with a heating rate of 5 °C/min), ash (NF EN 14, 775) and fixed carbon on a dry sample, which were made with the PerkinElmer TGA 4000 system were determined. Elementary analysis was made by energy-dispersive X-ray spectroscopy. The scanning electron microscopy (SEM) and the energy-dispersive X-ray spectroscopy (EDX) were made using a SEM Phenom Prox, phenomWorld Eindhoven. The SEM allowed us to examine the change in the physical structure of the activated carbon. The EDX gave us information on the presence and content of chemical elements on the material's surface. The iodine value corresponds to the quantity in milligrams of iodine adsorbed by one gram of activated carbon, when the residual concentration is 0.02 normal (CEFIC, 1986). It was determined using ASTM D4607–94 (ASTM International, 2006). The identification of crystalline materials was made by the X-ray diffraction method (XRD) using the Empyrean PANANALYTICAL diffractometer. Fourier-transform infrared spectroscopy (FTIR) by the Agilent Technology CARY 630 FTIR transmittance method was used to examine existing functional groups on the adsorbent surface. The specific surface area was estimated using the Brunauer-Emmett-Teller (BET) method using the Quantachrome Nova 4200e analyzer. BET surface and pore size and volume calculations were performed with NovaWin, version 11.03 using the Barett-Joyner-Halenda adsorption method (BJH).

2.4. Adsorption experiments

Adsorption tests were carried out in batch mode and under agitation in horizontal under room temperature (between 26 – 28 °C). This agitation method was chosen because magnetic agitation can destroy large grains during processing (Freihardt et al., 2017). The agitation speed adjusted to 230 rpm limits the diffusion of the film during the tests. On a fixed mass of activated carbon .., 50 mL of AMX (DCF) solution with concentration ranging 25 to 250 mg/L (20–200 mg/L) was put into agitation for a duration of 15 to 120 min (3 to 42 min). To make dimensionless the quantity of adsorbent put into solution, an adsorbate-adsorbent ratio (Eq. (2)) $R_{ads}$was defined, ranging from 0.025 to 0.25 g/g (0.02 to 0.2 g/g) for AMX (DCF).

$$R_{ads} = \frac{C_0 V}{1000 \times m_{CA}} \tag{2}$$

where R_{ads} is the adsorbate - adsorbent ratio (g/g), V the volum of the synthetic solution (L), m_{CA} the adsorbent mass (g), C_0 the initial concentration of the adsorbate (mg/L)

On each adsorbate, 10 tests were conducted at 25 mg/L (20 mg/L) and 15-minutes (3-minutes) intervals. The minimal concentration is function of the detection limit while the maximal concentration used is in the range of the concentrations found in pharmaceutical wastewater (Verma and Haritash, 2020; Xiong et al., 2019). Residual concentrations were determined by a UV-Visible spectrophotometer (DR. 5000 Hach Lange) at optimum wavelengths of 272 nm (276 nm) for AMX (DCF). These wavelengths obtained after scanning 200 to 800 nm, are consistent with the work of Chayid and Ahmed (2015), de Franco et al. (2018) and Tam et al. (2020). The following equation determined the quantities adsorbed at a time t.

$$q_t = \frac{(C_0 - C_t)V}{m_{CA}} \tag{3}$$

where q_t represents the adsorbed quantity (mg/g), C_0 and C_t the initial and residual concentration of the adsorbate at t time respectively (mg/L)

The different values $q_t$were used to determine the maximum adsorption applied to the Langmuir (Eq. (4)) and Freundlich (Eq. (5)) isotherms.Langmuir isotherm:

$$q_e = q_{\max}\frac{K_L C_e}{1 + K_L C_e}$$
$$thus\frac{C_e}{q_e} = \frac{1}{q_{\max}}C_e + \frac{1}{q_{\max}K_L} \tag{4}$$

Freundlich isotherm:

$$q_e = K_F C_e^{1/n}$$
$$thus \ln q_e = \frac{1}{n}\ln C_e + \ln K_F \tag{5}$$

where

$q_e, q_{\max}$

: adsorption capacity at equilibrium and Langmuir adsorption (mg/g), C_e : equilibrium concentration in the liquid phase (mg/L), n: Freundlich coefficient, K_L, K_F constant of Langmuir (L/mg) and Freundlich $(mg/g)(mg/L)^{\frac{-1}{n}}$

The linear isotherm $q_e = f(C_e)$was also drawn to define the significant adsorption ratios for studying the adsorption kinetics of the products. The adsorptions kinetics were obtained from the adsorption tests. The pseudo first-order model (Eq. (6)), pseudo second-order model (Eq. (7)) and the intra-particle diffusion model (Eq. (8)) were used to analyze experimental data of this kinetics.Pseudo first - order model:

$$\frac{dq_t}{dt} = K_1(q_e - q_t)$$
$$thus \ln(q_e - q_t) = \ln q_e - K_1 t \tag{6}$$

Pseudo second - order model:

$$\frac{dq_t}{dt} = K_2(q_e - q_t)^2$$
$$thus\frac{t}{q_t} = \frac{1}{q_e}t + \frac{1}{K_2 q_e^2} \tag{7}$$

Intra - particle diffusion model:

$$q_t = K_d t^{1/2} + C \tag{8}$$

where

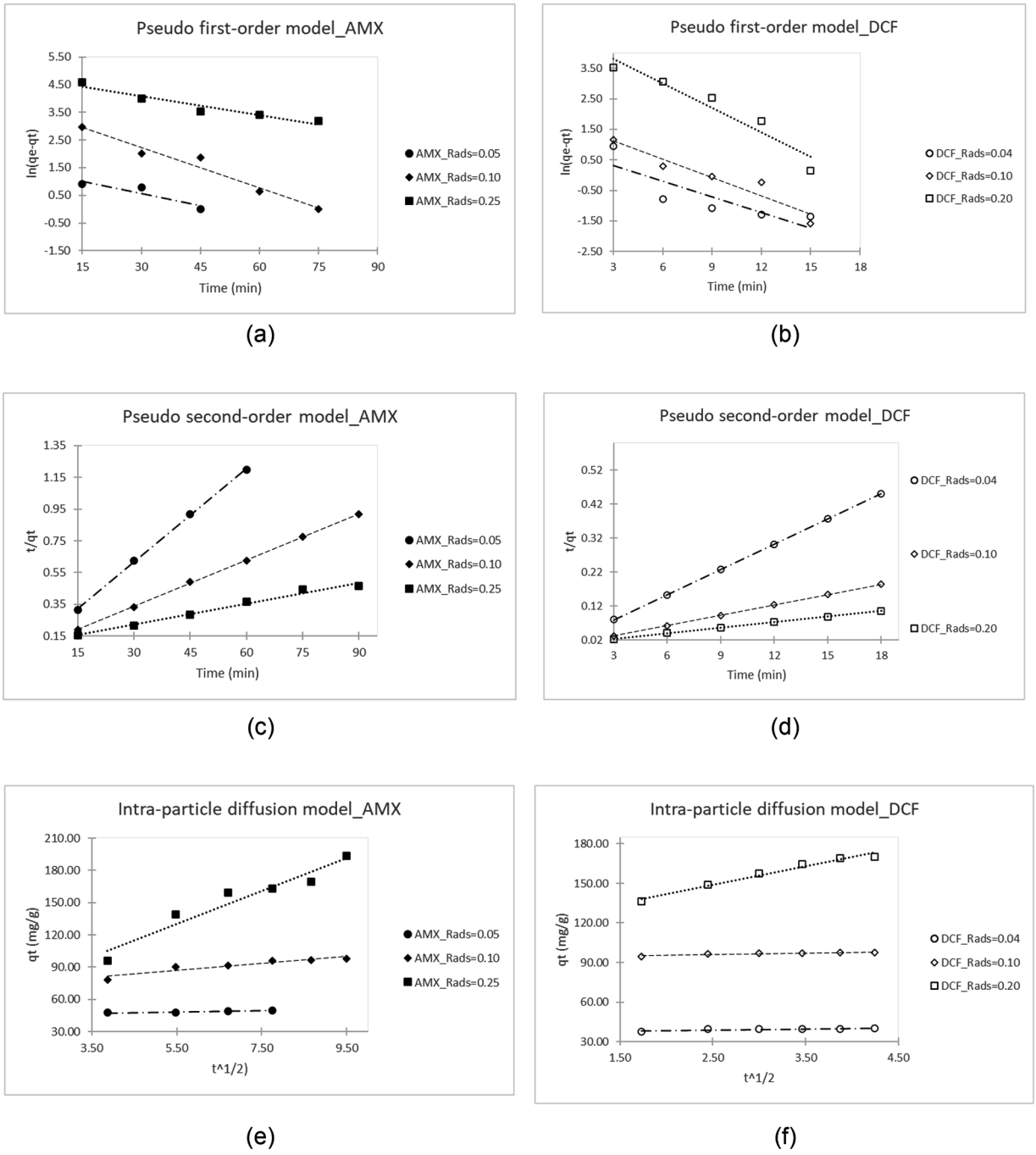

Fig. 6. Kinety models pseudo first-order (a) AMX, (b) DCF; pseudo second-order (c) AMX, (d) DCF; and intra-particle diffusion (e) AMX, (f) DCF.

K_1

, K_2, K_d : adsorption rate constant of pseudo first - order (1/min),pseudo second - order (g/mg.min) and intra - particle diffusion (mg/g.min$^{1/2}$) C: constant that gives an idea about the thickness of the boundary layer (mg/g)

3. Results and discussion

3.1. Modeling and optimization of activated carbon preparation

The experimental matrix and the results obtained are presented in Table 2. The different values of the iodine value are greater than those obtained on the same biomass activated with KOH by Tan et al., (2008b). Phosphoric acid would be more suitable for activating coconut shells than potassium hydroxide.

The regression model obtained by the RSM in coded variables is expressed by a second-degree polynomial (Eq. (3)):

$$Y = 835.4 + 85.9X_1 + 108.7X_2 - 138.9{X_1}^2 - 25.1{X_2}^2 + 3.2X_1X_2 \quad (9)$$

In this equation, the positive values of the coefficients show that the two factors considered have a synergistic effect on the response. Thus, the increase in the impregnation ratio and the temperature improves the availability of micropores which resulting in the different values of the iodine value. The same observations were made for their interaction. On the contrary, the second-order terms have an antagonistic effect, which means that very high values of the factors do not allow better availability of the pores. However, the effect of the interaction of factors

Table 9
Kinetic parameters of AMX and DCF adsorption.

Adsorbate	R_{ads}(g /g)	Models			
		Pseudo first-order model			
		q_{e-exp}(mg /g)	q_{e-th}(mg /g)	K_1(1 /min)	R^2
AMX	0.05	50.00	4.27	0.0296	0.8534
	0.10	97.83	40.00	0.0486	0.9630
	0.25	193.33	115.86	0.0225	0.9258
DCF	0.04	40.00	2.29	0.1713	0.7210
	0.10	97.81	5.62	0.2011	0.9138
	0.20	170.25	101.62	0.2681	0.9254
		Pseudo second-order model			
		q_{e-exp}(mg /g)	q_{e-th}(mg /g)	K_2(g /mg.min)	R^2
AMX	0.05	50.00	51.02	0.0132	0.9995
	0.10	97.83	103.09	0.0021	0.9996
	0.25	193.33	227.27	0.0002	0.9844
DCF	0.04	40.00	40.32	0.1337	0.9999
	0.10	97.81	98.04	0.0743	1
	0.20	170.25	181.82	0.0047	0.9994
		Intra-particle diffusion model			
		q_{e-exp}(mg /g)	q_{e-th}(mg /g)	K_d(mg /g.min$^{1/2}$)	R^2
AMX	0.05	50.00	49.75	0.6455	0.9051
	0.10	97.83	99.90	3.2622	0.8856
	0.25	193.33	191.61	15.3520	0.9307
DCF	0.04	40.00	40.29	0.8485	0.6781
	0.10	97.81	98.04	1.1702	0.8998
	0.20	170.25	173.38	14.0090	0.9751

(Fig. 2), indicates that the optimal iodine value field corresponds to $1.5 \leq IR \leq 2$ and a temperature above 650°C.

Table 3 presents the analysis of variance (ANOVA) of the obtained quadratic model (Eq. (3)). The Fisher value 20.32 associated with the *p −value* close to zero (therefore respecting the 95% confidence level) indicates that the model's description by second order quadratic regression is significant. Furthermore, based on the $p - value$, the statistically significant terms are the impregnation ratio, the activation temperature and the quadratic effect of the impregnation ratio.

The coefficient of determination $R^2 = 0.9355$ shows the excellent correlation that exists between the theoretical and experimental values. The difference between AdjR − squared and PredR − Squaredexceeds 0.2 means that the model can be reduced. Das and Mishra (2017) made the same observation particularly on the iodine value response to the RSM. However, this correlation is tolerable with the low value of the standard deviation corresponding to an acceptable coefficient of variation (CV = 7.24% ≤ 10%).

Under these conditions, the MINITAB 19 Statistical Software's optimal solution and the experimental results are presented in Table 4. The optimal conditions retained are IR = 1.66 and ActivationTemperature = 740°C for an optimum iodine value (930.28mg /g). Table 5 shows coconut shell and phosphoric acid as the best combination of coconut tree biomass and activated agent for iodine adsorption. Furthermore, the optimum recorded for this study is comparable with those reported in the literature from the same precursor and activated agent.

The activated carbon prepared under optimal conditions was characterized and then subjected to adsorption tests.

3.2. Characterization of raw biomass and activated carbon

3.2.1. Basic physicochemical properties

The results of the macromolecular composition and the ultimate and immediate analyzes are presented in Table 6. The main macromolecules are lignin and hemicellulose, which constitute the fractions that contribute the most to activated carbon production (Cagnon et al., 2009; Liyanage and Pieris, 2015). In general, the ultimate and immediate characteristics obtained are similar to those obtained during previous work on coconut shells (Kang et al., 2011; Ouyang et al., 2013). The phosphorus present in the elemental composition of activated carbon results from the impregnation with phosphoric acid. The apparent difference that is observed after activation of the lignocellulosic biomass is an indicator of the precursor quality and the effect of the activating agent (Mohd Iqbaldin et al., 2013). In fact, from the precursor to the activated carbon, the rate of volatile matter decreases while fixed carbon and ash increase. Thus, the carbonization considerably reduced the oxygen of the precursor, causing the significant presence of the mineral carbon. The hydrogen ratio obtained by Das et al., (2015) being substantially equal to the humidity of the sample analyzed. The absence of hydrogen observed in the present study is thought to be due to the activated carbon storage at 105 °C.

3.2.2. Intrinsic characterization of activated carbon

According to the SEM images obtained in Fig. 3.a, the prepared activated carbon has a good grain size between 50 and 250 μm. The image at 500x showed heterogeneous shape with pores and cavities that could easily be revealed above 1000x. These textural characteristics (Table 7) show a strong adsorption capacity of nitrogen. The average pore size indicates a co-presence of micropores and mesopores. The spectrum obtained from the FTIR (Fig. 3.b) gives information on the low heterogeneous chemical composition of the activated carbon. The low absorption peaks observed are generally due to decrease functional groups when switching from raw biomass to activated carbon (Chayid and Ahmed, 2015). However, the peaks observed around 2260 and 1699 correspond to the stretching C ≡ C of alkynes and C = Oaldehydes and carboxylic acids. The presence of these different groups is characteristic of activated carbons originated from coconut shells (Balogoun et al., 2015; Liyanage and Pieris, 2015). In addition, the crystallographic surface changes from raw biomass to adsorbent (Fig. 3.c). The peaks obtained at $2\theta = 18.00°$ and $2\theta = 22.39°$are characteristic of lignocellulosic materials (Keiluweit et al., 2010; Kim et al., 2011). The diffractogram of optimized activated carbon is similar to that obtained on activated carbon based on agricultural residues (Abdul Khalil et al., 2013; Kong et al., 2016). Thus, the two broad peaks observed at $2\theta = 23.93°$ (002) and $2\theta = 43.21°$ (100) testify to its amorphous character with a bit of crystalline structure. All these fundamental characteristics of activated carbon permit to test its adsorption potential.

3.3. Adsorption study

The two parameters that influence the adsorption are the contact time and the adsorbent dose. By substituting the residual concentration at equilibrium (C_e) by the residual rate of adsorbate at equilibrium ($Y_e = \frac{C_e}{C_0} \times 100$), the curve $R_{ads} = f(Y_e)$ follows the same shape as that of the linear isotherm $q_e = f(C_e)$ (Fig. 4.a). Thus, the increase of the adsorbate-adsorbent ratio results in a decrease in the removal efficiency. In other words, adsorption is more effective when the initial dose of absorbent (adsorbate) increases (decreases). Regarding the contact time, Figs. 4. b–c confirm the existence of an adsorption time plateau per pollutant concentration range (Boudrahem et al., 2017). For low initial concentrations of the adsorbent, equilibrium is reached quickly with a contact time varying between 15 and 90 min (3 and 18 min) for AMX (DCF). From $R_{ads} = 0.10 g/g$, the curve shows two stages: rapid adsorption followed by a slow phase until saturation. This is explained by the high availability of active surfaces which become saturated as adsorption increases. Similar observations have been made on the adsorption of trichlorophenol (Hameed et al., 2008) and methylene blue (Kong et al., 2016). The saturation time observed 90 min and 18 min respectively for AMX and DCF was considered as equilibrium time at $R_{ads} \geq 0.10$ for the drawing of the Langmuir and Freundlich isotherms (Figs. 5.a–b). The parameters of these isotherms are summarized in Table 8. The high values of the coefficient of determination R^2 indicate that the two models of isotherms can express adsorption behavior. However, the Langmuir isotherm better describes the adsorption of the two pharmaceutical molecules. This means that the adsorption occurs on a homogeneous surface and the adsorbates are distributed in a monolayer. The dimensionless separation factor between 0 and 1 proves that the adsorption of AMX and DCF on the prepared activated carbon is favorable. Likewise, the Freundlich coefficient with $1/n < 1$ confirms the adequacy of data adjustment by the Langmuir isotherm (Fytianos et al., 2000).

Fig. 4.a also indicates strategic values of R_{ads}. Complete elimination of AMX (DCF) is recorded for $R_{ads} \leq 0.075$ ($R_{ads} \leq 0.04$) while approximately 80% elimination corresponds to $R_{ads} = 0.25$ ($R_{ads} = 0.20$) for AMX (DCF). In addition, for $R_{ads} = 0.10$ an elimination of approximately 98% was recorded for both pharmaceutical molecules. Optimal adsorption of pharmaceutical pollutants might be possible with an adsorbate-absorbent ratio $R_{ads} = 0.10$. Furthermore, the kinetic study was carried out with these strategic values (Figs. 6.a-f). The results in Table 9 confirm that the pseudo second-order model best describes the adsorption of pharmaceutical pollutants (Baccar et al., 2012; Chayid and Ahmed, 2015). This model is based on chemical adsorption involving valence forces by sharing or exchanging electrons between adsorbent and adsorbate (Zhang et al., 2011). Depending on values of rate constant, the adsorption of diclofenac was faster than that of amoxicillin. It could be explained by the difference in molecular mass and the presence of radicals in their chemical structure. For the same adsorbate, the value of K_2 decreases with the increase of R_{ads} justifying the decrease in the removal efficiency with the rise in the initial concentration of adsorbate.

4. Conclusion

In this study, coconut shells were used as a precursor to prepare activated carbon using the chemical method of phosphoric acid activation. The response surface methodology has proven to be an effective method of determining the optimal conditions for the synthesis of activated carbon. The data analysis showed that a minimum temperature of 650 °C and a maximum impregnation rate IR = 2 promote strong iodine adsorption. However, the optimal solution from the central composite design corresponds to IR = 1.66 and Activation Temperature = 740°C for a maximum iodine value (930.28mg/g). The results of the physicochemical characterization confirm that the activated carbon prepared has a large microporous specific surface and a better adsorption capacity. The adsorption study was tested on two pharmaceutical substances: amoxicillin and diclofenac sodium. The influencing factors monitored were the contact time and the initial adsorbate - adsorbent ratio. A constant equilibrium contact time was observed for high initial concentrations and the removal efficiency depends mainly on R_{ads}. From isothermal and kinetic studies, it appears that the adsorption of the molecules studied satisfies the Langmuir isotherm and the pseudo second-order kinetic model. We noticed that diclofenac was faster adsorbed than amoxicillin. However, R_{ads}= 0.10 was the optimal condition for their adsorption. In this study, the experimentations were conducted in synthetic media. This can be considered as a limit of our research. Further research should focus on the adsorption behavior of more drugs on site, in order to validate optimal R_{ads} for pharmaceutical wastewater treatment by statistical modeling.

CRediT authorship contribution statement

Mohamed M. Arêmou Daouda: Conceptualization, Methodology, Formal analysis, Writing – original draft. **Akuemaho V. Onésime Akowanou:** Data curation, Visualization. **S. E. Reine Mahunon:** Validation, Resources. **Chris K. Adjinda:** Investigation. **Martin Pépin Aina:** Supervision. **Patrick Drogui:** Writing – review & editing.

Declaration of competing interest

The authors declare that they have no conflicts of interest.

References

Abdul Khalil, H.P.S., Jawaid, M., Firoozian, P., Rashid, U., Islam, A., Akil, H.M., 2013. Activated carbon from various agricultural wastes by chemical activation with KOH: preparation and characterization. J. Biobased Mater. Bioenergy 7, 708–714. https://doi.org/10.1166/jbmb.2013.1379.

As, D., Mh, K., Lr, M., 2015. Optimization of the process parameters for the preparation of activated carbon from low cost phoenix dactylifera using response surface methodology. Austin Chem. Eng. 2.

Asfaram, A., Ghaedi, M., Agarwal, S., Tyagi, I., Gupta, V.K., 2015. Removal of basic dye Auramine-O by ZnS:cu nanoparticles loaded on activated carbon: optimization of parameters using response surface methodology with central composite design. RSC Adv 5, 18438–18450. https://doi.org/10.1039/c4ra15637d.

A.S.T.M. International, 2006. Standard test method for determination of iodine number of activated carbon 1. www.astm.org 94, 1–5.

Azmi, N.B., Bashir, M.J.K., Sethupathi, S., Wei, L.J., Aun, N.C., 2015. Stabilized landfill leachate treatment by sugarcane bagasse derived activated carbon for removal of color, COD and NH3-N - Optimization of preparation conditions by RSM. J. Environ. Chem. Eng. 3, 1287–1294. https://doi.org/10.1016/j.jece.2014.12.002.

Baçaoui, A., Yaacoubi, A., Dahbi, A., Bennouna, C., Luu, R.P.T., Maldonado-Hodar, F.J., Rivera-Utrilla, J., Moreno-Castilla, C., 2001. Optimization of conditions for the preparation of activated carbons from olive-waste cakes. Carbon N. Y. 39, 425–432.

Baccar, R., Sarrà, M., Bouzid, J., Feki, M., Blánquez, P., 2012. Removal of pharmaceutical compounds by activated carbon prepared from agricultural by-product. Chem. Eng. J 211–212. https://doi.org/10.1016/j.cej.2012.09.099, 310–317.

Balogoun, C.K., Bawa, M.L., Osseni, S., 2015. Préparation des charbons actifs par voie chimique à l ' acide phosphorique à base de coque de noix de coco 9, 563–580.

Bazrafshan, E., Amirian, P., Mahvi, A.H., Ansari-Moghaddam, A., 2016. Application of adsorption process for phenolic compounds removal from aqueous environments: a systematic review. Glob. Nest J. 18, 146–163. https://doi.org/10.30955/gnj.001709.

Bestani, B., Benderdouche, N., Benstaali, B., Belhakem, M., Addou, A., 2008. Bioresource Technology Methylene blue and iodine adsorption onto an activated desert plant 99, 8441–8444. 10.1016/j.biortech.2008.02.053.

Boudrahem, N., Delpeux-Ouldriane, S., Khenniche, L., Boudrahem, F., Aissani-Benissad, F., Gineys, M., 2017. Single and mixture adsorption of clofibric acid, tetracycline and paracetamol onto Activated carbon developed from cotton cloth residue. Process Saf. Environ. Prot. 111, 544–559. https://doi.org/10.1016/j.psep.2017.08.025.

Budi, E., Nasbey, H., Bintoro, R.A., Wulandari, F., 2017. Activated coconut shell charcoal carbon using chemical-physical activation activated coconut shell charcoal carbon using chemical- physical activation 050003, 1–7. 10.1063/1.4941886.

Budnyak, T.M., Aminzadeh, S., Pylypchuk, I.V., Sternik, D., Tertykh, V.A., Lindström, M. E., Sevastyanova, O., 2018. Methylene blue dye sorption by hybrid materials from technical lignins. J. Environ. Chem. Eng. 6, 4997–5007. https://doi.org/10.1016/j.jece.2018.07.041.

Burakov, A.E., Galunin, E.V., Burakova, I.V., Kucherova, A.E., Agarwal, S., Tkachev, A. G., Gupta, V.K., 2018. Adsorption of heavy metals on conventional and nanostructured materials for wastewater treatment purposes: a review. Ecotoxicol. Environ. Saf. 148, 702–712. https://doi.org/10.1016/j.ecoenv.2017.11.034.

Busch, W., Schmidt, S., Kühne, R., Schulze, T., Krauss, M., Altenburger, R., 2016. Micropollutants in European rivers: a mode of action survey to support the development of effect-based tools for water monitoring. Environ. Toxicol. Chem. 35, 1887–1899. https://doi.org/10.1002/etc.3460.

Cagnon, B., Py, X., Guillot, A., Stoeckli, F., Chambat, G., 2009. Contributions of hemicellulose, cellulose and lignin to the mass and the porous properties of chars and steam activated carbons from various lignocellulosic precursors. Bioresour. Technol. 100, 292–298. https://doi.org/10.1016/j.biortech.2008.06.009.

CEFIC, 1986. Test-method-for-activated-carbon_86.pdf. Eur. Counc. Chem. Manuf. Fed.

Chayid, M.A., Ahmed, M.J., 2015. Amoxicillin adsorption on microwave prepared activated carbon from arundo donax linn: isotherms, kinetics, and thermodynamics studies. J. Environ. Chem. Eng. 3, 1592–1601. https://doi.org/10.1016/j.jece.2015.05.021.

Cizmas, L., Sharma, V.K., Gray, C.M., McDonald, T.J., 2015. Pharmaceuticals and personal care products in waters: occurrence, toxicity, and risk. Environ. Chem. Lett. 13, 381–394. https://doi.org/10.1007/s10311-015-0524-4.

Das, D., Samal, D.P., BC, M., 2015. Preparation of activated carbon from green coconut shell and its characterization. J. Chem. Eng. Process Technol. 06. https://doi.org/10.4172/2157-7048.1000248.

Das, S., Mishra, S., 2017. Box-Behnken statistical design to optimize preparation of activated carbon from limonia acidissima shell with desirability approach. J. Environ. Chem. Eng. 5, 588–600. https://doi.org/10.1016/j.jece.2016.12.034.

de Franco, M.A.E., de Carvalho, C.B., Bonetto, M.M., de Pelegrini Soares, R., Féris, L.A., 2018. Diclofenac removal from water by adsorption using activated carbon in batch mode and fixed-bed column: isotherms, thermodynamic study and breakthrough curves modeling. J. Clean. Prod. 181, 145–154. https://doi.org/10.1016/j.jclepro.2018.01.138.

Deblonde, T., Cossu-Leguille, C., Hartemann, P., 2011. Emerging pollutants in wastewater: a review of the literature. Int. J. Hyg. Environ. Health 214, 442–448. https://doi.org/10.1016/j.ijheh.2011.08.002.

Falås, P., Wick, A., Castronovo, S., Habermacher, J., Ternes, T.A., Joss, A., 2016. Tracing the limits of organic micropollutant removal in biological wastewater treatment. Water Res 95, 240–249. https://doi.org/10.1016/j.watres.2016.03.009.

Freihardt, J., Jekel, M., Ruhl, A.S., 2017. Comparing test methods for granular activated carbon for organic micropollutant elimination. J. Environ. Chem. Eng. 5, 2542–2551. https://doi.org/10.1016/j.jece.2017.05.002.

Freitas, J.V., Nogueira, F.G.E., Farinas, C.S., 2019. Coconut shell activated carbon as an alternative adsorbent of inhibitors from lignocellulosic biomass pretreatment. Ind. Crops Prod. 137, 16–23. https://doi.org/10.1016/j.indcrop.2019.05.018.

Fytianos, K., Voudrias, E., Kokkalis, E., 2000. Sorption-desorption behaviour of 2,4-dichlorophenol by marine sediments. Chemosphere 40, 3–6. https://doi.org/10.1016/S0045-6535(99)00214-3.

Georgin, J., Dotto, G.L., Mazutti, M.A., Foletto, E.L., 2016. Preparation of activated carbon from peanut shell by conventional pyrolysis and microwave irradiation-pyrolysis to remove organic dyes from aqueous solutions. J. Environ. Chem. Eng. 4, 266–275. https://doi.org/10.1016/j.jece.2015.11.018.

Godin, B., Agneessens, R., Goffot, S., Lamaudière, S., Sinnaeve, G., Gerin, P.A., Delcarte, J., 2011. Revue bibliographique sur les méthodes d'analyse des polysaccharides structuraux des biomasses lignocellulosiques. Biotechnol. Agron. Soc. Environ. 15, 165–182.

González-García, P., 2018. Activated carbon from lignocellulosics precursors: a review of the synthesis methods, characterization techniques and applications. Renew. Sustain. Energy Rev. 82, 1393–1414. https://doi.org/10.1016/j.rser.2017.04.117.

González-Pleiter, M., Gonzalo, S., Rodea-Palomares, I., Leganés, F., Rosal, R., Boltes, K., Marco, E., Fernández-Piñas, F., 2013. Toxicity of five antibiotics and their mixtures towards photosynthetic aquatic organisms: implications for environmental risk assessment. Water Res 47, 2050–2064. https://doi.org/10.1016/j.watres.2013.01.020.

Gratuito, M.K.B., Panyathanmaporn, T., Chumnanklang, R., 2008. Production of activated carbon from coconut shell : optimization using response surface methodology 99, 4887–4895. 10.1016/j.biortech.2007.09.042.

Gueye, M., Richardson, Y., Kafack, F.T., Blin, J., 2014. High efficiency activated carbons from African biomass residues for the removal of chromium(VI) from wastewater. J. Environ. Chem. Eng. 2, 273–281. https://doi.org/10.1016/j.jece.2013.12.014.

Hameed, B.H., Tan, I.A.W., Ahmad, A.L., 2008. Adsorption isotherm, kinetic modeling and mechanism of 2,4,6-trichlorophenol on coconut husk-based activated carbon. Chem. Eng. J. 144, 235–244. https://doi.org/10.1016/j.cej.2008.01.028.

Heidarinejad, Z., Dehghani, M.H., Heidari, M., Javedan, G., Ali, I., Sillanpää, M., 2020. Methods for preparation and activation of activated carbon: a review. Environ. Chem. Lett. 18, 393–415. https://doi.org/10.1007/s10311-019-00955-0.

Hui, T.S., Abbas, M., Zaini, A., 2015. Potassium hydroxide activation of activated carbon : a commentary. 10.5714/CL.2015.16.4.275.

Itodo, A.U., Abdulrahman, F.W., Hassan, L.G., Maigandi, S.A., Itodo, H.U., 2010. Application of methylene blue and iodine adsorption in the measurement of specific surface area by four acid and salt treated activated carbons . 3, 25–33.

Jawad, A.H., Bardhan, M., Islam, Atikul, Islam, Azharul, Syed-hassan, S.S.A., Surip, S.N., Bardhan, M., Islam, Atikul, Islam, Azharul, Syed-hassan, S.S.A., Surip, S.N., 2020. Insights into the modeling, characterization and adsorption performance of mesoporous activated carbon from corn cob residue via microwave- assisted H3PO4 activation. Surfaces and Interfaces.

Jawad, A.H., Ishak, M.A.M., Farhan, A.M., Ismail, K., 2017a. Response surface methodology approach for optimization of color removal and COD reduction of methylene blue using microwave-induced NaOH activated carbon from biomass waste. Desalin. Water Treat. 62, 208–220. https://doi.org/10.5004/dwt.2017.20132.

Jawad, A.H., Rashid, R.A., Ishak, M.A.M., Wilson, L.D., 2016. Adsorption of methylene blue onto activated carbon developed from biomass waste by H2SO4 activation: kinetic, equilibrium and thermodynamic studies. Desalin. Water Treat. 57, 25194–25206. https://doi.org/10.1080/19443994.2016.1144534.

Jawad, A.H., Rashid, R.A., Ismail, K., Sabar, S., 2017b. High surface area mesoporous activated carbon developed from coconut leaf by chemical activation with H3PO4 for adsorption of methylene blue. Desalin. Water Treat. 74, 326–335. https://doi.org/10.5004/dwt.2017.20571.

Jawad, A.H., Rashid, R.A., Mahmuod, R.M.A., Ishak, M.A.M., Kasim, N.N., Ismail, K., 2015. Adsorption of methylene blue onto coconut (Cocos nucifera) leaf: optimization, isotherm and kinetic studies. Desalin. Water Treat. 57, 8839–8853. https://doi.org/10.1080/19443994.2015.1026282.

Jodeh, S., Abdelwahab, F., Jaradat, N., Warad, I., Jodeh, W., 2016. Adsorption of diclofenac from aqueous solution using Cyclamen persicum tubers based activated carbon (CTAC). J. Assoc. Arab Univ. Basic Appl. Sci. 20, 32–38. https://doi.org/10.1016/j.jaubas.2014.11.002.

Kang, S., Jian-chun, J., Dan-dan, C., 2011. Preparation of activated carbon with highly developed mesoporous structure from Camellia oleifera shell through water vapor gasification and phosphoric acid modification. Biomass and Bioenergy 35, 3643–3647. https://doi.org/10.1016/j.biombioe.2011.05.007.

Keiluweit, M., Nico, P.S., Johnson, M., Kleber, M., 2010. Dynamic molecular structure of plant biomass-derived black carbon (biochar). Environ. Sci. Technol. 44, 1247–1253. https://doi.org/10.1021/es9031419.

Kim, P., Johnson, A., Edmunds, C.W., Radosevich, M., Vogt, F., Rials, T.G., Labbé, N., 2011. Surface functionality and carbon structures in lignocellulosic-derived biochars produced by fast pyrolysis. Energy and Fuels 25, 4693–4703. https://doi.org/10.1021/ef200915s.

Kong, W., Zhao, F., Guan, H., Zhao, Y., Zhang, H., Zhang, B., 2016. Highly adsorptive mesoporous carbon from biomass using molten-salt route. J. Mater. Sci. 51, 6793–6800. https://doi.org/10.1007/s10853-016-9966-8.

Kovalova, L., Siegrist, H., Von Gunten, U., Eugster, J., Hagenbuch, M., Wittmer, A., Moser, R., McArdell, C.S., 2013. Elimination of micropollutants during post-treatment of hospital wastewater with powdered activated carbon, ozone, and UV. Environ. Sci. Technol. 47, 7899–7908. https://doi.org/10.1021/es400708w.

Lesaoana, M., Mlaba, R.P.V., Mtunzi, F.M., Klink, M.J., Edijike, P., Pakade, V.E., 2019. Influence of inorganic acid modification on Cr(VI) adsorption performance and the physicochemical properties of activated carbon. South African J. Chem. Eng. 28, 8–18. https://doi.org/10.1016/j.sajce.2019.01.001.

Li, S., Han, K., Li, J., Li, M., Lu, C., 2017. Preparation and characterization of super activated carbon produced from gulfweed by KOH activation. Microporous Mesoporous Mater 243, 291–300. https://doi.org/10.1016/j.micromeso.2017.02.052.

Liang, Q., Liu, Y., Chen, M., Ma, L., Yang, B., Li, L., Liu, Q., 2020. Optimized preparation of activated carbon from coconut shell and municipal sludge. Mater. Chem. Phys. 241. https://doi.org/10.1016/j.matchemphys.2019.122327.

Liyanage, C.D., Pieris, M., 2015. A Physico-chemical analysis of coconut shell powder. Procedia Chem 16, 222–228. https://doi.org/10.1016/j.proche.2015.12.045.

Luo, Y., Guo, W., Ngo, H.H., Nghiem, L.D., Hai, F.I., Zhang, J., Liang, S., Wang, X.C., 2014. A review on the occurrence of micropollutants in the aquatic environment and their fate and removal during wastewater treatment. Sci. Total Environ. 619–641. https://doi.org/10.1016/j.scitotenv.2013.12.065, 473–474.

Maddodi, S.A., Alalwan, H.A., Alminshid, A.H., Abbas, M.N., 2020. Isotherm and computational fluid dynamics analysis of nickel ion adsorption from aqueous solution using activated carbon. South African J. Chem. Eng. 32, 5–12. https://doi.org/10.1016/j.sajce.2020.01.002.

Mahmood, N.A.J., Abdulmajeed, Y.R., 2017. Adsorption of amoxicillin onto activated carbon from aqueous solution. Int. J. Curr. Eng. Technol. 7, 62–67.

Mailler, R., Gasperi, J., Coquet, Y., Derome, C., Buleté, A., Vulliet, E., Bressy, A., Varrault, G., Chebbo, G., Rocher, V., 2016. Removal of emerging micropollutants from wastewater by activated carbon adsorption: experimental study of different activated carbons and factors influencing the adsorption of micropollutants in wastewater. J. Environ. Chem. Eng. 4, 1102–1109. https://doi.org/10.1016/j.jece.2016.01.018.

Mailler, R., Gasperi, J., Patureau, D., Vulliet, E., Delgenes, N., Danel, A., Deshayes, S., Eudes, V., Guerin, R., 2017. Fate of emerging and priority micropollutants during the sewage sludge treatment : case study of Paris conurbation . Part 1 : contamination of the different types of sewage sludge. Waste Manag 59, 379–393. https://doi.org/10.1016/j.wasman.2016.11.010.

Margot, J., Kienle, C., Magnet, A., Weil, M., Rossi, L., de Alencastro, L.F., Abegglen, C., Thonney, D., Chèvre, N., Schärer, M., Barry, D.A., 2013. Treatment of micropollutants in municipal wastewater: ozone or powdered activated carbon? Sci. Total Environ. 461–462. https://doi.org/10.1016/j.scitotenv.2013.05.034, 480–498.

Marsh, H., Rodriguez-Reinoso, F., 2006. Activated Carbon. Elsevier. Elsevier, Amsterdam; London.

Miguet, M., Goetz, V., Plantard, G., Jaeger, Y., 2016. Sustainable thermal regeneration of spent activated carbons by solar energy: application to water treatment. Ind. Eng. Chem. Res. 55, 7003–7011. https://doi.org/10.1021/acs.iecr.6b01260.

Mohd Iqbaldin, M.N., Khudzir, I., Mohd Azlan, M.I., Zaidi, A.G., Surani, B., Zubri, Z., 2013. Properties of coconut shell activated carbon. J. Trop. For. Sci. 25, 497–503.

Moussavi, G., Alahabadi, A., Yaghmaeian, K., Eskandari, M., 2013. Preparation, characterization and adsorption potential of the NH4Cl-induced activated carbon for the removal of amoxicillin antibiotic from water. Chem. Eng. J. 217, 119–128. https://doi.org/10.1016/j.cej.2012.11.069.

Nayl, A.E.A., Elkhashab, R.A., El Malah, T., Yakout, S.M., El-Khateeb, M.A., Ali, M.M.S., Ali, H.M., 2017. Adsorption studies on the removal of COD and BOD from treated

sewage using activated carbon prepared from date palm waste. Environ. Sci. Pollut. Res. 24, 22284–22293. https://doi.org/10.1007/s11356-017-9878-4.

Nekouei, F., Nekouei, S., Tyagi, I., Gupta, V.K., 2015. Kinetic, thermodynamic and isotherm studies for acid blue 129 removal from liquids using copper oxide nanoparticle-modified activated carbon as a novel adsorbent. J. Mol. Liq. 201, 124–133. https://doi.org/10.1016/j.molliq.2014.09.027.

Ouyang, S., Xu, S., Song, N., Jiao, S., 2013. Coconut shell-based carbon adsorbents for ventilation air methane enrichment. Fuel 113, 420–425. https://doi.org/10.1016/j.fuel.2013.06.004.

Pasquini, L., Munoz, J.F., Pons, M.N., Yvon, J., Dauchy, X., France, X., Le, N.D., France-Lanord, C., Görner, T., 2014. Occurrence of eight household micropollutants in urban wastewater and their fate in a wastewater treatment plant. Statistical evaluation. Sci. Total Environ. 481, 459–468. https://doi.org/10.1016/j.scitotenv.2014.02.075.

Patnukao, P., Pavasant, P., 2008. Activated carbon from Eucalyptus camaldulensis Dehn bark using phosphoric acid activation. Bioresour. Technol. 99, 8540–8543. https://doi.org/10.1016/j.biortech.2006.10.049.

Pellerin, N., 2002. Technique de Van Soest pour la détermination des constituants pariétaux de végétaux à l'analyse des produits de compostage et litières diverses à usage agronomique . Principe Mode opératoire. Note Tech. NT01-01. Fich. NTVansoest.doc 1–15.

Putra, E.K., Pranowo, R., Sunarso, J., Indraswati, N., Ismadji, S., 2009. Performance of activated carbon and bentonite for adsorption of amoxicillin from wastewater: mechanisms, isotherms and kinetics. Water Res 43, 2419–2430. https://doi.org/10.1016/j.watres.2009.02.039.

Rashid, R.A., Jawad, A.H., Ishak, M.A.M., Kasim, N.N., 2016. KOH-activated carbon developed from biomass waste: adsorption equilibrium, kinetic and thermodynamic studies for Methylene blue uptake. Desalin. Water Treat. 57, 27226–27236. https://doi.org/10.1080/19443994.2016.1167630.

Senthilkumar, T., Chattopadhyay, S.K., Miranda, L.R., 2017. Optimization of activated carbon preparation from pomegranate peel (Punica granatum Peel) using RSM. Chem. Eng. Commun. 204, 238–248. https://doi.org/10.1080/00986445.2016.1262358.

Shao, Y., Chen, Z., Hollert, H., Zhou, S., Deutschmann, B., Seiler, T.B., 2019. Toxicity of 10 organic micropollutants and their mixture: implications for aquatic risk assessment. Sci. Total Environ. 666, 1273–1282. https://doi.org/10.1016/j.scitotenv.2019.02.047.

Suhas, Gupta, V.K., Carrott, P.J.M., Singh, R., Chaudhary, M., Kushwaha, S., 2016. Cellulose: a review as natural, modified and activated carbon adsorbent. Bioresour. Technol. 216, 1066–1076. https://doi.org/10.1016/j.biortech.2016.05.106.

Sun, K., Leng, C.Y., Jiang, J.C., Bu, Q., Lin, G.F., Lu, X.C., Zhu, G.Z., 2017. Microporous activated carbons from coconut shells produced by self-activation using the pyrolysis gases produced from them, that have an excellent electric double layer performance. New Carbon Mater 32, 451–459. https://doi.org/10.1016/S1872-5805(17)60134-3.

Sun, Y., Li, H., Li, G., Gao, B., Yue, Q., Li, X., 2016. Characterization and ciprofloxacin adsorption properties of activated carbons prepared from biomass wastes by H3PO4 activation. Bioresour. Technol. 217, 239–244. https://doi.org/10.1016/j.biortech.2016.03.047.

Tam, N.T.M., Liu, Y., Bashir, H., Yin, Z., He, Y., Zhou, X., 2020. Efficient removal of diclofenac from aqueous solution by potassium ferrate-activated porous graphitic biochar: ambient condition influences and adsorption mechanism. Int. J. Environ. Res. Public Health 17, 1–22. https://doi.org/10.3390/ijerph17010291.

Tan, I.A.W., Ahmad, A.L., Hameed, B.H., 2008a. Preparation of activated carbon from coconut husk : optimization study on removal of 2, 4, 6-trichlorophenol using response surface methodology. J. Hazard. Mater. 153, 709–717. https://doi.org/10.1016/j.jhazmat.2007.09.014.

Tan, I.A.W., Ahmad, A.L., Hameed, B.H., 2008b. Optimization of preparation conditions for activated carbons from coconut husk using response surface methodology. Chem. Eng. J. 137, 462–470. https://doi.org/10.1016/j.cej.2007.04.031.

Telegang Chekem, C., 2017. Elaboration De Matériaux Composites Bifonctionnels Charbon actif-TiO2 à Partir Des Ressources Végétales Tropicales Pour Des Applications De Traitement De L'eau Par Voie solaire. PhD Thesis. Univ. Perpignan Via Domitia.

Tomul, F., Arslan, Y., Başoğlu, F.T., Babuçcuoğlu, Y., Tran, H.N., 2019. Efficient removal of anti-inflammatory from solution by Fe-containing activated carbon: adsorption kinetics, isotherms, and thermodynamics. J. Environ. Manage. 238, 296–306. https://doi.org/10.1016/j.jenvman.2019.02.088.

Vargas, A.M.M., Garcia, C.A., Reis, E.M., Lenzi, E., Costa, W.F., Almeida, V.C., 2010. NaOH-activated carbon from flamboyant (Delonix regia) pods : optimization of preparation conditions using central composite rotatable design. Chem. Eng. J. 162, 43–50. https://doi.org/10.1016/j.cej.2010.04.052.

Verma, M., Haritash, A.K., 2020. Photocatalytic degradation of Amoxicillin in pharmaceutical wastewater: a potential tool to manage residual antibiotics. Environ. Technol. Innov. 20. https://doi.org/10.1016/j.eti.2020.101072.

Xiong, T., Yuan, X., Wang, H., Wu, Z., Jiang, L., Leng, L., 2019. Highly e ffi cient removal of diclofenac sodium from medical wastewater by Mg /Al layered double hydroxide-poly (m-phenylenediamine) composite. Chem. Eng. J. 366, 83–91. https://doi.org/10.1016/j.cej.2019.02.069.

Yang, B., Liu, Y., Liang, Q., Chen, M., Ma, L., Li, L., Liu, Q., Tu, W., Lan, D., Chen, Y., 2019. Evaluation of activated carbon synthesized by one-stage and two-stage co-pyrolysis from sludge and coconut shell. Ecotoxicol. Environ. Saf. 170, 722–731. https://doi.org/10.1016/j.ecoenv.2018.11.130.

Zhang, C.L., Qiao, G.L., Zhao, F., Wang, Y., 2011. Thermodynamic and kinetic parameters of ciprofloxacin adsorption onto modified coal fly ash from aqueous solution. J. Mol. Liq. 163, 53–56. https://doi.org/10.1016/j.molliq.2011.07.005.